Computational Materials Science 115 (2016) 72–76

Contents lists available at ScienceDirect

Computational Materials Science

journal homepage: www.elsevier.com/locate/commatsci

Energy absorption induced oscillation of a rotating curved carbon nanotube in a nano bearing

Zhaoliang Gao [a], Haifang Cai [b], Jing Wan [b], Kun Cai [b,c,*]

[a] Institute of Soil and Water Conservation, Northwest A&F University, Yangling 712100, China
[b] College of Water Resources and Architectural Engineering, Northwest A&F University, Yangling 712100, China
[c] Research School of Engineering, The Australian National University, Canberra, ACT 2601, Australia

ARTICLE INFO

Article history:
Received 15 November 2015
Received in revised form 12 December 2015
Accepted 17 December 2015
Available online 2 February 2016

Keywords:
Nano device
Carbon nanotube
Curved tube
Transmission system
Resonance

ABSTRACT

In a nano bearing, a curved inner carbon nano tube (CNT) constrained by two short outer CNTs will have an oscillation along the curved axis of the tube when a specified rotational velocity is input on one end of the inner tube. It is found that the free end has periodic axial translational oscillation and the amplitude of oscillation is very high when the frequency of the input rotational velocity is close to an eigen/resonance frequency of the system, i.e., energy absorption of the inner tube from the interaction between the inner and outer tubes. Higher curvature of the inner tube leads to higher value of fundamental frequency of the system. The free end of the inner tube also has obvious torque oscillation. Both of the axial translational oscillation and torque oscillation of the free end can be used as output signals of the system as working in a nano signal generator. The mid part of the inner tube, i.e., the part between two outer tubes, has obvious in-plane vibration, which indicates that the present nano bearing is a two-dimensional device.

1. Introduction

With the decreasing of the sizes of components in a micro-electro-mechanical system (MEMS), both of theoretical study and development of experiment techniques on design of a nano-electro-mechanical system (NEMS) become urgent in recent years. Due to excellent physical properties, carbon nano structures, e.g., carbon nanotube (CNT) [1–3], graphene sheet [4,5], carbon nano-scroll [6,7], etc., attract much attention in the studies. In particular, CNT-based oscillator/bearing/motor is one of the new conceptual designs of NEMS.

By experiments on axial tension of inner tube in multi-walled carbon nanotubes (MWCNTs), Cumings and Zettl [2] test the inter-shell friction force and find that the extruded core can be retracted inside the outer tubes quickly when the core is released. They explain that the van der Waals force drives the retraction, and demonstrate a possible path to construct a gigahertz-frequency oscillator. Zheng and Jiang [8] propose the mechanical model of such nano oscillator. Following the finding, a series of investigations have been made to give a design of the nano device. For example, Legoas et al. [9] research the stability of the nano oscillator with molecular dynamics (MD) simulations.

Many experimentalists try to fabric such nano device [2,10–12]. However, up to now, there is no one nano device with size of only few nanometers. The reason is that the energy dissipation is serious during relative motion between adjacent tubes and a long-time stable motion cannot be easily maintained. Using MD simulations, Zhao et al. [13] imply that the friction phenomenon between two adjacent CNTs is the major reason for the transmission of orderly translational kinetic energy into disorderly thermal vibrational energy. As can be seen, the damping behavior still exists even in short-tube oscillators (see Fig. 1c in Ref. [13]). Guo et al. [14] compare the energy dissipation rates between commensurate and incommensurate double-walled CNT (DWCNT)-based oscillators. Their results show that the inter-tube friction is proportional to energy dissipation rate, but inversely proportional to the oscillation frequency. In a long-tube oscillator, the damping oscillation is very clear [15]. Cook et al. [16] find that friction within a rotating CNT bearing is proportional to relative rotating speed and system temperature, but slightly depends on the length and mean diameter of inner tube. Hence, to obtain a nano oscillator/motor with controllable amplitude or frequency, the energy dissipation due to inter-tube friction should be made up by absorbing energy from environment. For example, Neild et al. [17] suggest to using periodic forces to excite the oscillation meeting the conditions of controllability. Kang et al. [18] try to find a frequency-controlled CNT-based oscillator, which is made from three co-axial CNTs,

* Corresponding author at: Research School of Engineering, The Australian National University, Canberra, ACT 2601, Australia
E-mail address: kuncai99@163.com (K. Cai).

http://dx.doi.org/10.1016/j.commatsci.2015.12.028
0927-0256/

i.e., two outer tubes and one inner tube. By adjusting the gap between two outer tubes, the oscillation of the inner tube behaves differently. Either external electricity field or non-uniform heating method can also be adopted to drive a nano rotary/linear motor. For example, Fennimore et al. [10] choose the MWCNTs as a key motion-enabling component in a nano electricity-driven actuator. Bourlon et al. [11] attach a plate on the MWCNTs-based bearing, which is driven to rotate by a charged stator. By experiments, Barreiro et al. [12] find the axial motion of a cargo on a movable CNT relative to another coaxial CNT with axial thermal gradient. Further study on thermal-gradient driven motion is given by other researchers [19–22]. Peculiarly, Cai et al. [23] find that the uniform temperature field can also drive the rotation of a DWCNTs-based motor.

From the forgoing review, few work demonstrates the oscillation and simultaneous rotation of the movable component in a nano motor. Recently, Cai et al. [24] find that the high-speed rotating inner tube in a fixed outer tube can be excited to oscillate periodically. The mechanism is that the rotational kinetic energy of inner tube becomes into both of thermal vibration energy of system and axial translational kinetic energy of inner tube. This finding indicates that a stable oscillation can also be obtained when the inner tube has a stable rotational speed.

Different from both of the work by Kang et al. [18] and Cai et al. [23], in the present study, we propose a new rotation–oscillation transmission system from DWCNTs. But in the present model, the inner tube is curved [25–32] and constrained in two short outer tubes. Giving a specified rotational speed on one end of the inner tube, the other tube end has different dynamic response. MD simulations are carried out to show the dynamic response.

2. Models and methods

Three models for the system shown in Fig. 1b–d are considered: Model 1: curvature radius of R = 5.161 nm when n = 128; Model 2: R = 8.019 nm when n = 164; and Model 3: R = 11.194 nm when n = 204.

The molecular dynamic (MD) simulation is carried out using LAMMPS [33]. In simulation, the AIREBO potential [34] is adopted to indicate the interaction of the carbon atoms in system. The time integral increment is 1 fs. Before simulation, 400 ps of Nosé–Hoover bath at canonical (NVT) ensemble with T = 300 K is applied on the system for relaxation. During relaxation, the top 4 layers of the upper right end of the inner tube are fixed. The two outer tubes are fixed, too. After relaxation, the input rotational frequency is applied on the lower left end of the curved inner tube, and the value of gap, output rotational frequency and the potential of inner tube are output.

To find the influence of the input rotational frequency of the inner tube on the dynamic response of system, the value of ω_{in}, is set to be 20, 50, 80, 120 and 150 GHz, respectively.

3. Results and discussions

From either *potential history* curve or *output rotation history* curve in Table 1, one can find that the system tends to be stable after ~2 ns. The wild fluctuation of the output signals of system in the initial stage is mainly due to the sudden application of the input rotation of the curved inner tube. After 2 ns, most of the output signals keep stable. Two characters of the output signals are necessary to be demonstrated. One is the damping behavior. The other is the stable large amplitude vibration of the upper right end of the curved inner tube.

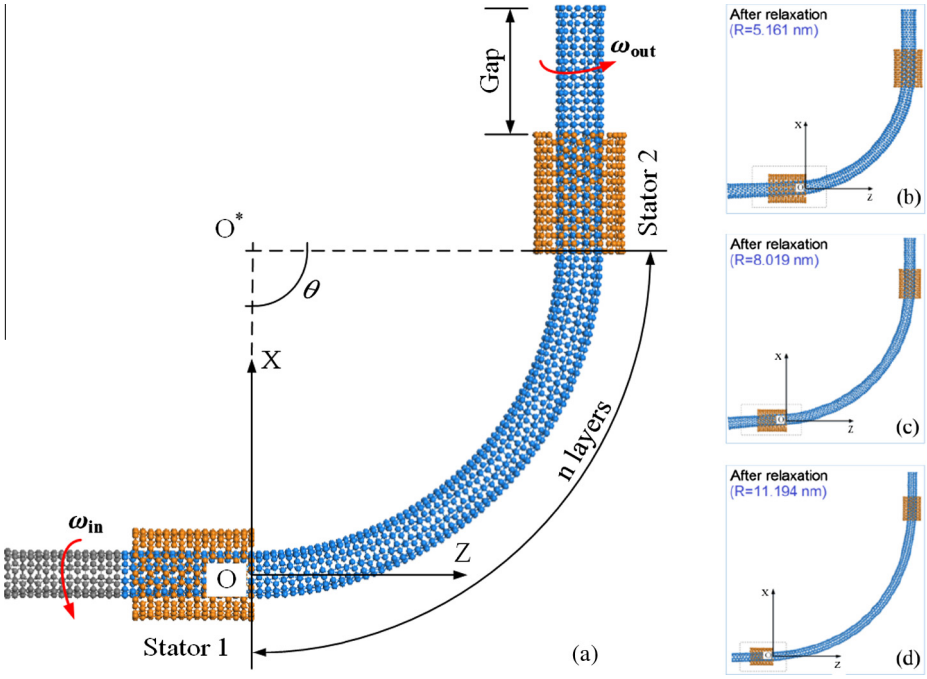

Fig. 1. (a) The initial simulation model for a nano rotation–oscillation transmission system, in which the two straight 16-layer outer (10, 10) carbon tubes (orange parts) are fixed. Initially, there are 16 layers of atoms on each end of the inner tube beyond the constraint of the stators. The lower left end (grey part, 16-layer) of the curved inner (5, 5) carbon nanotube has a constant input rotational speed, i.e., ω_{in}, and the upper right end has an output rotational frequency, i.e., ω_{out}. The value of gap is the axial distance between the upper right end of the inner tube and stator 2. Between the two outer tubes, the mid part of the inner tube with n layers is curved. And the radius of the curved axis, i.e., R, is the distance between O and O*. θ is the central angle, and equal 90° in this study. After relaxation (b, c and d), near stator 1, the inner tubes do not keep co-axial with the outer tubes and the included angle is ~2° (see the sections within dashed boxes). (For interpretation of the references to color in this figure legend, the reader is referred to the web version of this article.)

Table 1
Dynamic response of the system with different model parameters and input rotational speeds (ω_{in}) within [0, 4] ns.

Gap history	Potential energy history	Output rotation history
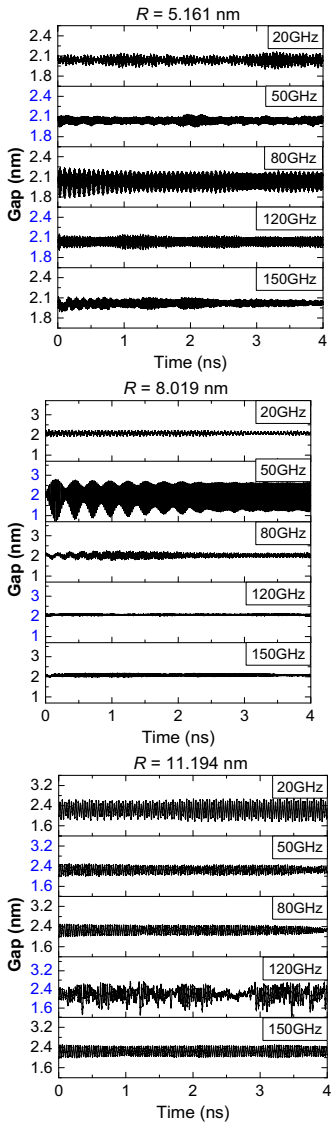	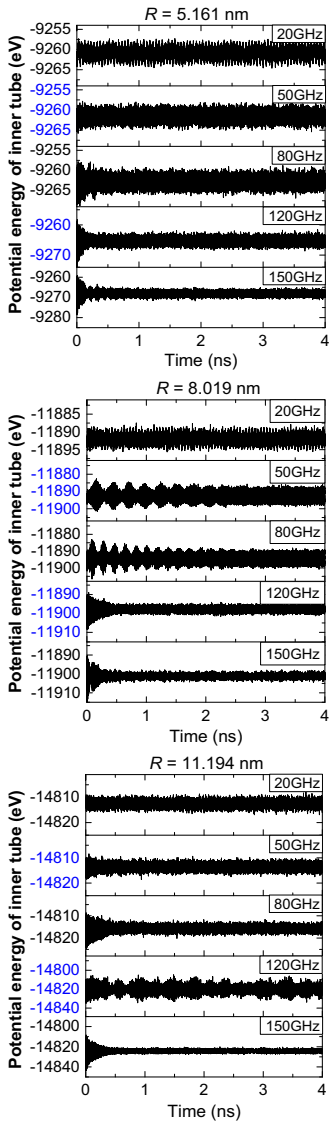	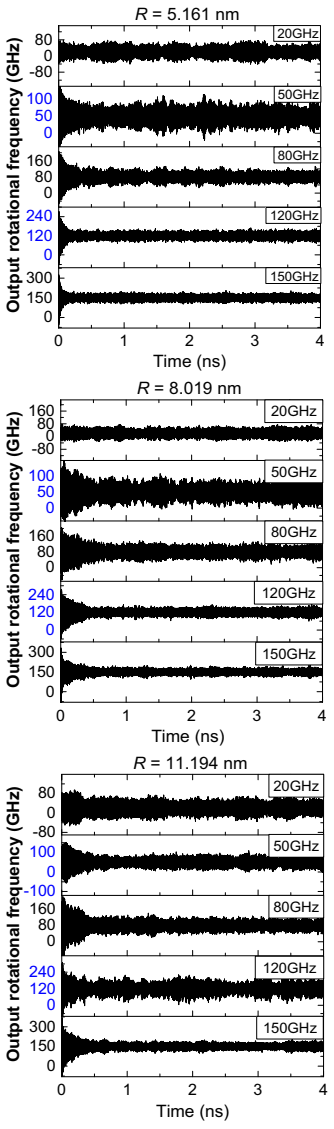

As we know, the *potential energy* of the inner tube depends on two factors, i.e., the number of covalently bonded atoms and the deformation of tube. Therefore, from the mid column in Table 1 one can find that the potential fluctuates obviously in the first 2 ns. The fluctuation is caused by two factors: the thermal vibration of atoms, and the large deformation of the inner tube.

In the right column in Table 1, the value of *output rotational frequency* of the inner tube is also fluctuating during simulation. But the mean value (on time average) of the frequency always equals the input rotational frequency. It indicates that the inner tube is not damaged under distortion. After 2 ns of simulation, the fluctuation of the output rotational frequency tends to be stable, and the amplitudes are ~**51.66**, 26.22, 36.78, 29.63 and 31.50 GHz in Model 1 with five different input rotational speeds (20, 50, 80, 120 and 150 GHz), respectively. It implies that *the upper right end of the inner tube has drastic torsional oscillation during simulation*. For Model 2 and Model 3, one can find the torsional oscillation, as well.

Before demonstrating the stable vibration of the *gap* (or the upper right end of the inner tube with large amplitude), the mechanism for the vibration should be given. When the lower left end of the curved inner tube rotates, the rest part of the curved tube is driven to rotate because the strong interaction within the shell, i.e., the sp^2 carbon–carbon bonds can keep the whole curved tube undamaged. If the shell is curved, the axial/longitudinal distance between the atoms on the shell varies periodically. Therefore, the vibration of the shell exists along its generatrix direction. If the two ends of the curved inner tube are constrained rigidly, the amplitude of such vibration will be negligible. However, in a real system, the curved inner tube is constrained by two straight outer tubes. The interaction between the inner tube and stators is the van der Waals (vdW) force among the atoms on tubes. And the vdW force is sensitive to the relative positions of atoms. Simultaneously, the curved tube tends to be straight (Fig. 1b, c and d). Hence, the curved inner tube is subjected to a non-equilibrium transversal vdW force from the lower left outer tube. It leads to variation of the curvature of the inner tube locally. This is the reason for the vibration of the upper right end of the inner tube when a constant rotational speed is applied on the lower left end of the inner tube.

To demonstrate the vibration of the inner tube exited by input rotation, Fig. 2 gives five snapshots of Model 2 (R = 8.019 nm) with

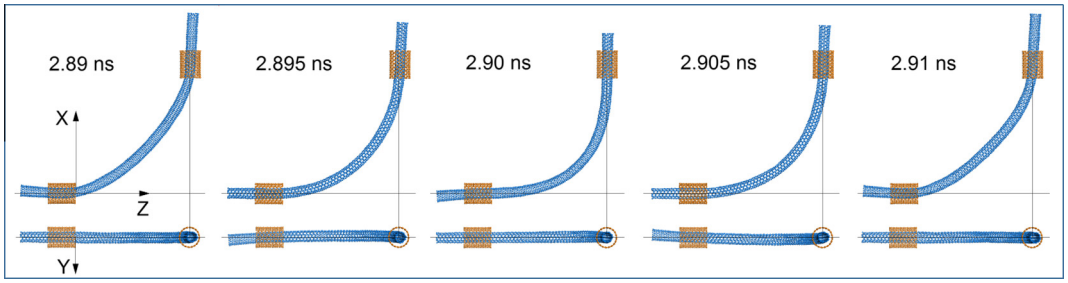

Fig. 2. Snapshots of Model 2 (R = 8.019 nm) and $\omega_{in} = 50$ GHz during [2.89, 2.91] ns. The top layer lists front views (in xz-plane) of configurations at different time. The lower layer lists vertical views (in yz-plane) of configurations.

$\omega_{in} = 50$ GHz. From 2.89 ns to 2.91 ns, the inner tube has a period of vibration. Because the lower left end of the inner tube cannot move axially and the axial length of the tube keeps approximately unchanged, the mid-part of the inner tube between the two fixed outer tubes has different length and different curvature during vibration. Obviously, the included angle between this part and the outer tube varies at the same time. Therefore, the vdW interaction between the inner tube and the outer tubes also shows periodic. The lower layer in Fig. 2 shows that the inner tube has very slight vibration in yz-plane. It indicates that the inner tube behaves perfect toughness during rotation along its curved axis. The reason is that the bending stiffness of the inner tube in yz-plane is much greater than the shearing stiffness of the tube in xz-plane in the present system. It also hints that the present nano bearing is a two-dimensional device.

Meanwhile, the friction between the inner tube and the outer tubes leads to the damping vibration of the curved inner tube (e.g., the history curve of gap at the situation of R = 8.019 nm and $\omega_{in} = 50$ GHz in Table 1).

When the system is in a stable state, the periodic vibration of gap can be considered as an output signal of the system. And the amplitude of gap fluctuation, which can be considered as axial oscillation of the upper right end of the curved inner tube, in the same model varies with the value of ω_{in}. For example, in Fig. 3, which gives the dynamic response of the system within [2.8, 3.0] ns, the amplitudes of gap in Model 1 (R = 5.161 nm) are ~0.084, 0.044, **0.122**, 0.063 and 0.045 nm when $\omega_{in} = 20$, 50, 80, 120 and 150 GHz, respectively. Obviously, the amplitude with respect to $\omega_{in} = 80$ GHz in Model 1 is the highest one among the five cases. Similarly, the amplitudes of gap in Model 2 (R = 8.019 nm) are ~0.067, **0.710**, 0.102, 0.013 and 0.052 nm for five input rotational speeds, respectively. And 0.710 nm with respect to $\omega_{in} = 50$ GHz in Model 2 is the greatest among the five cases. In Model 3 (R = 11.194 nm), the amplitudes of gap are ~**0.397**, 0.203, 0.224, **0.605** and 0.243 nm for five input rotational speeds, respectively. The amplitudes with respect to $\omega_{in} = 20$ and 120 GHz are much larger than those of the other three cases. It is concluded that the amplitude of gap fluctuation depends on the input rotational frequency and the value of R. Therefore, the input rotational frequency of the curved inner tube which has the highest amplitude of gap must be very close to one of the eigen/resonance frequencies of the dynamic system. And we call $\omega_{in} = 80$ GHz is an approximate eigen frequency (AEF) of Model 1 (R = 5.161 nm), or $\omega_{in} = 50$ GHz of Model 2 (R = 8.019 nm). It is known that the resonance of the inner tube is actually due to the energy absorption of the inner tube from interaction between the tubes. Hence, oscillation of the upper right end of the inner tube is caused by energy absorption. For Model 3 (R = 11.194 nm), both of 20 and 120 GHz are as AEFs. One can find that the system with lower value of R has a higher value of AEF. The reason is that the inner tubes in the three models have the same chirality and the outer tubes are also identical, the stiffness of the system with lower value of R is higher and, therefore, the AEF is higher.

The curve (Model 2 with $\omega_{in} = 50$ GHz in Fig. 3) also indicates that the signal in the modulated carrier transmission (MCT) with period of ~0.03 ns. The period is of ~0.05 ns for the MCT (in the rectangle frame) in Model 1 or Model 2 with $\omega_{in} = 20$ GHz.

Fig. 4a gives the histories of gap of Model 2 with different values of input rotational frequency. When the input rotational frequency varies from 42 to 58 GHz, the curves fluctuate differently. The amplitude of gap with respect to 44 GHz is much lower than that of 46 GHz curve. From 46 to 58 GHz, the amplitude decreases monotonously. To demonstrate the character of amplitudes of

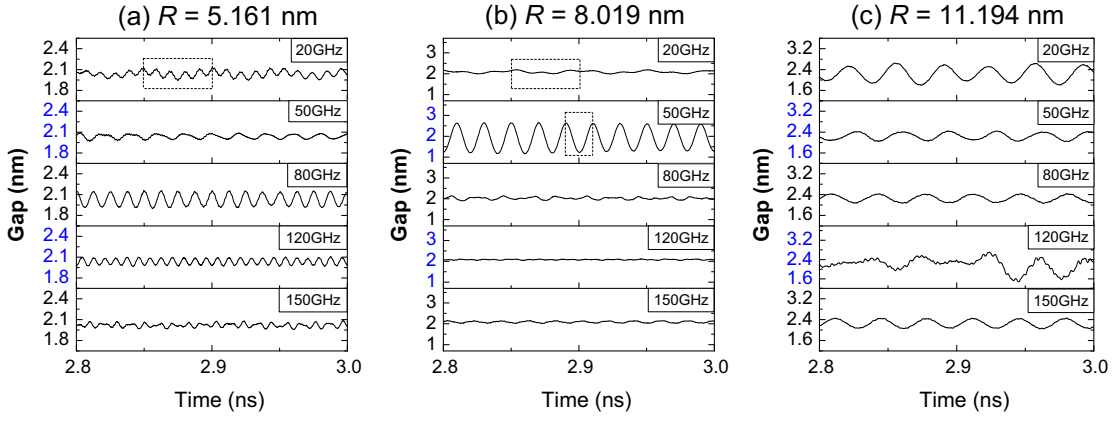

Fig. 3. History curves of gap and potential energy of the inner tube in the three models during [2.8, 3.0] ns. (a) Model 1, R = 5.161 nm; (b) Model 2, R = 8.019 nm; (c) Model 3, R = 11.194 nm.

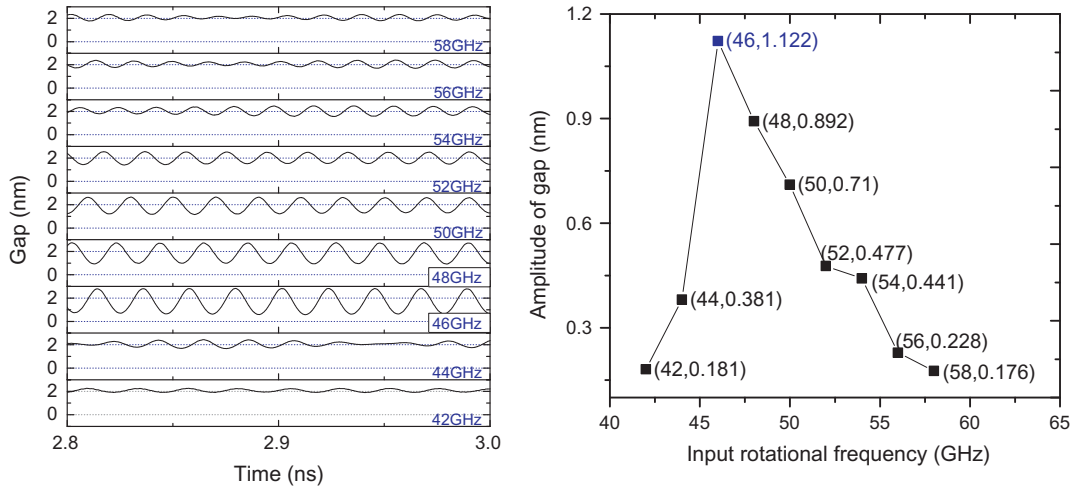

(a) History during [2.8, 3.0] ns (b) Amplitude

Fig. 4. Histories of gap and amplitudes of gap in Model 2 with respect to input rotational frequency during [2.8, 3.0] ns.

gap in Model 2 with different input rotational frequencies, we calculate the average amplitudes of gap during [2.8, 3.0] ns (in Fig. 4a) and show them in Fig. 4b. As can be seen, the maximum of amplitude is 1.122 nm with respect to $\omega_{in} = 46$ GHz, which is obviously larger than 0.710 nm with respect to 50 GHz. Hence, we conclude that 46 GHz is much closer to the eigen frequency than 50 GHz.

4. Conclusions

From numerical computation, the oscillation behavior of the curved rotary inner tube in the bearing from CNTs is investigated. Some remarkable conclusions can be drawn.

(1) Inputting a rotational frequency on one end of the curved inner tube, the other end (free end) of the inner tube will output not only the rotation but also the axial translational oscillation and torque oscillation.
(2) The amplitude of axial translational oscillation depends on the difference between the input rotational frequency and the eigen/resonance (serious energy absorption state) frequency of the system, lower difference leads to higher amplitude. Higher curvature of the mid part of the inner tube has higher fundamental frequency.
(3) The oscillation of the inner tube happens within the plane where the curved inner tube is layout. Hence, the nano bearing is a two-dimensional device.
(4) The output signals, e.g., oscillation and rotation of the free end of the inner tube, behave as MCTs, which implies a potential application in design of a nano signal generator.

Appendix A. Supplementary material

Supplementary data associated with this article can be found, in the online version, at http://dx.doi.org/10.1016/j.commatsci.2015.12.028.

References

[1] S. Iijima, Nature 354 (1991) 56.
[2] J. Cumings, A. Zettl, Science 289 (2000) 602.
[3] R. Zhang, Z. Ning, Y. Zhang, Q. Zheng, Q. Chen, H. Xie, Q. Zhang, W. Qian, F. Wei, Nat. Nanotechnol. 8 (2013) 912.
[4] K.S. Novoselov, A.K. Geim, S.V. Morozov, D. Jiang, Y. Zhang, S.V. Dubonos, I.V. Grigorieva, A.A. Firsov, Science 306 (2004) 666.
[5] J. Feng, W. Li, X. Qian, J. Qi, L. Qi, J. Li, Nanoscale 4 (2012) 4883.
[6] Z.P. Xu, M.J. Buehler, ACS Nano 4 (2010) 3869.
[7] U. Mirsaidov, V.R.S.S. Mokkapati, D. Bhattacharya, H. Andersen, M. Bosman, B. Özyilmaz, P. Matsudaira, Lab Chip 13 (2013) 2874.
[8] Q.S. Zheng, Q. Jiang, Phys. Rev. Lett. 88 (2002) 045503.
[9] S.B. Legoas, V.R. Coluci, S.F. Braga, P.Z. Coura, S.O. Dantas, D.S. Galvão, Phys. Rev. Lett. 90 (2003) 055504.
[10] A. Fennimore, T. Yuzvinsky, W.Q. Han, M. Fuhrer, J. Cumings, A. Zettl, Nature 424 (2003) 408.
[11] B. Bourlon, D.C. Glattli, C. Miko, L. Forró, A. Bachtold, Nano Lett. 4 (2004) 709.
[12] A. Barreiro, R. Rurali, E.R. Hernandez, J. Moser, T. Pichler, L. Forro, A. Bachtold, Science 320 (2008) 775.
[13] Y. Zhao, C.C. Ma, G.H. Chen, Q. Jiang, Phys. Rev. Lett. 91 (2003) 175504.
[14] W. Guo, Y. Guo, H. Gao, Q. Zheng, W. Zhong, Phys. Rev. Lett. 91 (2003) 125501.
[15] J.L. Rivera, C. McCabe, P.T. Cummings, Nanotechnology 16 (2) (2005) 186.
[16] E.H. Cook, M.J. Buehler, Z.S. Spakovszky, J. Mech. Phys. Solids 61 (2013) 652.
[17] A. Neild, T.W. Ng, Q. Zheng, Europhys. Lett. 87 (2009) 16002.
[18] J.W. Kang, K. Kim, H.J. Hwang, O.K. Kwon, Phys. Lett. A 374 (2010) 3658.
[19] H.A. Zambrano, J.H. Walther, R.L. Jaffe, J. Chem. Phys. 131 (2009) 241104.
[20] Q.Q. Hou, B.Y. Cao, Z.Y. Guo, Nanotechnology 20 (2009) 495503.
[21] P.M. Shenai, Z.P. Xu, Y. Zhao, Nanotechnology 22 (2011) 485702.
[22] I. Santamaria-Holek, D. Reguera, J.M. Rubi, J. Phys. Chem. C 117 (2013) 3109.
[23] K. Cai, Y. Li, Q.H. Qin, H. Yin, Nanotechnology 25 (2014) 505701.
[24] K. Cai, H. Yin, Q.H. Qin, Y. Li, Nano Lett. 14 (2014) 2558.
[25] H. Üstünel, D. Roundy, T.A. Arias, Nano Lett. 5 (2005) 523.
[26] W. Xia, L. Wang, Comput. Mater. Sci. 49 (2010) 99.
[27] A. Eichler, J. Moser, M.I. Dykman, A. Bachtold, Nat. Commun. 4 (2013) 2843.
[28] M.M.S. Fakhrabadi, P.K. Khorasani, A. Rastgoo, M.T. Ahmadian, Solid State Commun. 157 (2013) 38.
[29] K. Cai, H.F. Cai, J. Shi, Q.H. Qin, Appl. Phys. Lett. 106 (2015) 241907.
[30] S. Imani Yengejeh, João M.P.Q. Delgado, Antonio G. Barbosa de Lima, A. Öchsner, Adv. Mater. Sci. Eng. 2014 (2014) 815340.
[31] S. Imani Yengejeh, S.A. Kazemi, A. Öchsner, Mechanical and Materials Engineering of Modern Structure and Component Design, Advanced Structured Materials, Springer International Publishing, vol. 70, 2015, pp. 401–412.
[32] S. Imani Yengejeh, A. Öchsner, Proceedings of the Institution of Mechanical Engineers, Part N: Journal of Nanoengineering and Nanosystems, vols. 1–9, SAGE Publications, 2015, http://dx.doi.org/10.1177/1740349915579713.
[33] LAMMPS Molecular Dynamics Simulator, 2013, <http://lammps.sandia.gov/>.
[34] S.J. Stuart, A.B. Tutein, J.A. Harrison, J. Chem. Phys. 112 (2000) 6472.